Neuropsychopharmacology (2016) 41, 802–810

www.neuropsychopharmacology.org

Cognitive Deficits in Calsyntenin-2-deficient Mice Associated with Reduced GABAergic Transmission

Tatiana V Lipina[1,2,6], Tuhina Prasad[3,6], Daisaku Yokomaku[3,6], Lin Luo[3,6], Steven A Connor[3,4], Hiroshi Kawabe[5], Yu Tian Wang[4], Nils Brose[5], John C Roder[1] and Ann Marie Craig*[,3]

[1]Lunenfeld Tanenbaum Research Institute, Mount Sinai Hospital, Toronto, ON, Canada; [2]Federal State Budgetary Scientific Institution, Scientific Research Institute of Physiology and Basic Medicine, Novosibirsk, Russia; [3]Brain Research Centre and Department of Psychiatry, University of British Columbia, Vancouver, BC, Canada; [4]Brain Research Centre and Department of Medicine, University of British Columbia, Vancouver, BC, Canada; [5]Department of Molecular Neurobiology, Max Planck Institute for Experimental Medicine, Göttingen, Germany

Calsyntenin-2 has an evolutionarily conserved role in cognition. In a human genome-wide screen, the *CLSTN2* locus was associated with verbal episodic memory, and expression of human calsyntenin-2 rescues the associative learning defect in orthologous *Caenorhabditis elegans* mutants. Other calsyntenins promote synapse development, calsyntenin-1 selectively of excitatory synapses and calsyntenin-3 of excitatory and inhibitory synapses. We found that targeted deletion of calsyntenin-2 in mice results in a selective reduction in functional inhibitory synapses. Reduced inhibitory transmission was associated with a selective reduction of parvalbumin interneurons in hippocampus and cortex. *Clstn2*$^{-/-}$ mice showed normal behavior in elevated plus maze, forced swim test, and novel object recognition assays. However, *Clstn2*$^{-/-}$ mice were hyperactive in the open field and showed deficits in spatial learning and memory in the Morris water maze and Barnes maze. These results confirm a function for calsyntenin-2 in cognitive performance and indicate an underlying mechanism that involves parvalbumin interneurons and aberrant inhibitory transmission.
Neuropsychopharmacology (2016) **41,** 802–810; doi:10.1038/npp.2015.206; published online 12 August 2015

INTRODUCTION

Calsyntenin-2, also known as alcadein-γ, is a neuronal cell surface synaptic protein with an evolutionarily conserved role in learning and memory. In humans, *CLSTN2* encoding calsyntenin-2 was identified in a genome-wide screen for memory-related variants in cognitively normal cohorts (Papassotiropoulos *et al*, 2006). *CLSTN2* alleles were associated with significant differences in delayed word recall, reflecting episodic hippocampus-dependent memory. Association of *CLSTN2* alleles with verbal memory was replicated in adolescents (Jacobsen *et al*, 2009), and association with semantic memory and global cognitive performance was found in an old age population (Laukka *et al*, 2013). Further, *CLSTN2* and *KIBRA* showed interactive effects on verbal episodic memory (Pantzar *et al*, 2014; Preuschhof *et al*, 2010). Such interactive effects may explain why association of *CLSTN2* alleles with episodic memory was not seen in all cohorts (Papassotiropoulos *et al*, 2006). An influence of *CLSTN2* allele on memory is supported by neuroimaging data. *CLSTN2* genotype associated with the level of functional connectivity between right parahippocampal gyrus, bilateral caudate nuclei, and frontal cortical regions recruited during verbal recognition (Jacobsen *et al*, 2009). *CLSTN2* was independently reported to affect temporal lobe volume (Kohannim *et al*, 2012). Furthermore, mutations in the *Caenorhabditis elegans* ortholog, *CASY-1*, result in learning deficits in multiple paradigms (Hoerndli *et al*, 2009; Ikeda *et al*, 2008), and expression of human calsyntenin-2 rescues the associative learning defect of *CASY-1* mutants (Hoerndli *et al*, 2009).

Despite this evidence for a conserved role of calsyntenin-2 in cognitive function, calsyntenin-2 is poorly characterized in terms of molecular interactions and cellular function, and information on a calsyntenin-2-deficient mouse model has been lacking. All three calsyntenins share a similar domain structure, with extracellular cadherin and LNS domains and an intracellular calcium-binding domain, and all undergo prominent ectodomain cleavage (Araki *et al*, 2004). Calsyntenin-2 mRNA is expressed in a brain-specific manner with high levels in hippocampal CA2-CA3 pyramidal neurons, dentate gyrus hilar neurons, presumptive interneurons throughout cortex and hippocampus, olfactory bulb mitral cells and cerebellar Purkinje cells, and at a moderate level in many cortical layer 5-6 pyramidal cells (Hintsch *et al*, 2002). All calsyntenin proteins were observed to be localized at postsynaptic sites (Hintsch *et al*, 2002).

*Correspondence: Dr AM Craig, Brain Research Centre, University of British Columbia, Room F149, 2211 Wesbrook Mall, Vancouver, BC V6T 2B5, Canada, Tel: +604 822 7283, Fax: +604 822 7299, E-mail: acraig@mail.ubc.ca
[6]These authors contributed equally to this work.
Received 18 November 2014; revised 5 June 2015; accepted 1 July 2015; accepted article preview online 14 July 2015

Mice with targeted deletions in the other calsyntenin family members exhibit deficits in synapse development. Hippocampal neurons of *Clstn1*$^{-/-}$ mice show a delay in maturation of excitatory synapses and dendrite arbors (Ster *et al*, 2014) related to the interaction of calsyntenin-1 with kinesin-1 light chain and a vesicular transport function (Araki *et al*, 2007; Konecna *et al*, 2006). Hippocampal neurons of *Clstn3*$^{-/-}$ mice show reductions in excitatory and inhibitory synapse density and synaptic transmission related to the interaction of calsyntenin-3 with the synaptic organizing protein α-neurexin and synaptogenic function (Pettem *et al*, 2013). In contrast, calsyntenin-2 lacks synaptogenic activity and did not bind neurexin in similar assays as were used for calsyntenin-3 (Pettem *et al*, 2013), and a vesicular transport function has not been reported for calsyntenin-2 as for calsyntenin-1. Thus, calsyntenin family members may have distinct functions.

To assess the role of calsyntenin-2 in brain function, we generated and characterized mice with a targeted deletion in *Clstn2*. The results presented here confirm roles for calsyntenin-2 in cognitive function and brain development, specifically in development of inhibitory synapses and parvalbumin interneurons.

MATERIALS AND METHODS

Generation of *Clstn2*$^{-/-}$ Mice

All animal procedures were approved by the institutional Animal Care Committees and were conducted in compliance with state guidelines, the Canadian Council on Animal Care, and the Russian Academy of Science based on ECC Directive 86/609/EEC. The *Clstn2* locus was targeted by homologous recombination in 129/Ola embryonic stem cells as detailed in the Supplementary Data. The mutant allele was backcrossed for at least nine generations with C57BL/6 J mice.

Antibodies

Antibodies against calsyntenin-2 were raised in rabbits (Covance) against GST fusions with the cytosolic domain (RVRIA…INIWK for C-terminal antibody) or membrane-proximal extracellular domain (ISCLQ…QVLHH for N-terminal antibody) expressed from the pGEX-4T-1 vector and purified from bacteria. The antibody against calsyntenin-1 was raised against a GST fusion with a membrane-proximal extracellular domain (IDCLY…EVLHL). The antibody against calsyntenin-3 and calsyntenin expression vectors were described previously (Pettem *et al*, 2013). Primary antibodies were used for tissue immunofluorescence against: MAP2 (chicken polyclonal IgY; 1:2000; Abcam ab5392); VGluT1 (rabbit, 1:1000; Synaptic Systems 135 302); GAD65 (mouse IgG2a, 1:100, GAD-6-c, Developmental Studies Hybridoma Bank); parvalbumin (mouse IgG1, 1:4000; Sigma P3088); somatostatin (rat IgG2b, 1:1000, Millipore MAB354); calretinin (mouse IgG1, 1:1000, Millipore MAB1568); and calbindin (mouse IgG1,1:1000, Swant 300).

Tissue Immunofluorescence and Image Analysis

For immunofluorescence studies, brain tissue samples were collected from P30 *Clstn2*$^{-/-}$ and littermate wild-type (WT) male mice. The mice were anesthetized with 20% urethane and perfused transcardially with cold PBS followed by 4% paraformaldehyde with 4% sucrose in PBS (pH 7.4). The brains were post-fixed in cold 4% paraformaldehyde in PBS overnight. The brains were then cryoprotected in 30% sucrose in PBS at 4°C and frozen in OCT (Tissue-Tek; Sakura-Finetek) using dry ice. Coronal cryostat sections (20 μm) were cut at hippocampal level and mounted on Superfrost Plus slides. Sections for analysis were chosen at approximately interaural 1.74 mm, bregma − 2.06 mm. The sections were incubated in blocking solution (5% BSA+5% normal goat serum+0.25% Triton X100 in PBS) for 1 h then incubated overnight (or 60 h for somatostatin staining) at 4 °C with primary antibodies diluted in blocking solution. Sections were washed in PBS and incubated for 1 h at room temperature with the appropriate secondary antibodies conjugated to Alexa 488, 568 or 647 (Molecular Probes/Invitrogen). Sections were washed in PBS containing the nuclear counterstain DAPI (4′,6 diamidino-2-phenylindole), and mounted in elvanol (Tris-HCl, glycerol, and polyvinyl alcohol with 2% 1,4-diazabi-cyclo[2,2,2]octane).

All image acquisition and analysis was performed with the experimenter blind to genotype. Quantification of excitatory (VGluT1) and inhibitory (GAD65) synaptic markers as well as parvalbumin positive terminals was performed on a minimum of six sections per animal from 3–5 pairs of *Clstn2*$^{-/-}$ and WT mice for each region. Digital images were captured using a Zeiss LSM 700 confocal microscope at × 40 magnification with × 3 zoom using customized filters. Puncta were defined by an intensity threshold, and total integrated intensity of puncta were measured. For interneuron cell counts, images were captured on an Olympus FluoView 1000 or Zeiss LSM 700 confocal microscope using a × 10 lens. Images were viewed in Photoshop (Adobe) and cell counts were performed manually. Analysis was performed using Metamorph 6.1 (Molecular Devices), Image J, Excel (Microsoft), and Prism (GraphPad Software). All data are reported as the mean ± SEM.

Electrophysiology

Clstn2$^{-/-}$ mice and WT littermates (6–10-week old) were killed following a cervical dislocation and brains were placed in ice-cold slicing solution consisting of (in mM): 120 NMDG, 2.5 KCl, 1.2 NaH_2PO_4, 25 $NaHCO_3$, 1.0 $CaCl_2$, 7.0 $MgCl_2$, 2.4 Na-pyruvate, 1.3 Na-ascorbate, 20 D-glucose with pH adjusted to 7.35 using HCl acid (unless stated, all chemicals and drugs were purchased from Sigma or BioShop, Canada). The hippocampus was dissected out and sliced in the transverse plane (400 μm thickness) using a manual tissue chopper (Stoelting). Slices were collected in ACSF composed of (in mM): 124 NaCl, 3 KCl, 1.25 NaH_2PO_4, 1 $MgSO_47H_2O$, 2 $CaCl_2$, 26 $NaHCO_3$ and 15 D-glucose bubbled continuously with carbogen (95%O_2/5% CO_2) to maintain the pH at 7.3, for 1 h at 30 °C then 30 min at room temperature. For recording, slices were sampled randomly from the entire dorsal ventral axis. Slices were transferred to a submerged chamber and continuously perfused with carbogenated ACSF (2–3 ml/min) at room temperature. Whole-cell recordings of CA1 pyramidal neurons were performed using the 'blind' method with a MultiClamp 700B amplifier. For miniature excitatory

postsynaptic current (mEPSC) recordings, cells were voltage clamped at −60 mV in the presence of tetrodotoxin (TTX; 500 nM; Ascent Scientific) and bicuculline methiodide (10 μM; Abcam). Recording pipettes were filled with solution containing (in mM): 122.5 Cs-methanesulfonate, 17.5 CsCl, 2 $MgCl_2$, 10 EGTA, 10 HEPES, 4 ATP (K), and 5 QX-314, with pH adjusted to 7.2 by CsOH. For mIPSC recordings, cells were voltage clamped at −70 mV in the presence of TTX (500 nM), CNQX (10 μM), DL-AP5 (50 μM) and the recording pipette was filled with solution containing (in mM): 140 CsCl, 0.1 $CaCl_2$, 2 $MgCl_2$, 10 HEPES, 10 EGTA, and 4 ATP(K), with pH adjusted to 7.2 using CsOH. WinLTP in continuous acquisition mode was used for recording. Analyses for frequency and amplitude were conducted using MiniAnalysis software. Statistical analyses were completed using GraphPad InStat and SigmaPlot.

Behavioral Experiments

Clstn2 mutant mice were maintained on a 12 h light/dark cycle (lights on at 0700 h) with *ad libitum* food and water. Behavioral tests were done between 0900 and 1600 h on adult mice (2–4 months of age). The behavioral equipment was cleaned with 70% ethanol between mice to remove residual odors. All behavioral testing procedures were conducted from less aversive to more stressful tests, separated by 3–5 days from each other. Experiments were performed with the experimenter blind to genotype. For the open-field and forced swim tests, behavioral data for males and females were pooled and analyzed together due to the lack of sex effects. Only males were tested in the elevated plus maze, Morris water maze, Barnes maze, and object recognition tests. Details of the elevated plus maze and forced swim test are presented in Supplementary Data.

Open Field

Each mouse was placed in the middle of a directly illuminated (200 Lux) automated activity cage (42 cm × 42 cm × 30 cm; Accuscan Instruments). Travel distance was measured over 30 min and time in the center over 5 min.

Morris Water Maze

The water maze consisted of a 185-cm diameter cylindrical tank that contained a 15-cm circular platform and water (26 ± 1 °C) rendered opaque by the addition of white nontoxic paint. Cues were placed on each wall of the room, including a colorful (1 m tall) plastic toy wagon jutting from the wall, a checker board (1 m × 1 m), a blue fitness ball (75 cm in diameter), and a cross of black stripes (each stripe 1.5 m × 30 cm). The task was performed as described (Saab *et al*, 2011) with minor modifications. Mice were released randomly from one out of five points far from the escape platform. The training regime consisted of a training session to a visible platform on the first day and then to a submerged platform in the northeast quadrant for 4 days (four trials per day; maximum duration 90 s; inter-trial interval 30 min). Subjects not able to find the platform during acquisition trials were directed by the experimenter to its location and left resting there for 10 s before being removed from the pool. A retention trial (90 s) with the platform removed from the pool was performed 24 h after the last acquisition trial.

Barnes Maze

The Barnes maze was performed essentially as described (Han *et al*, 2014). The maze is a planar, round white plywood platform (122 cm diameter) with 40 evenly spaced holes (5 cm diameter) located 4 cm from the edge. Spatial cues with distinct patterns and shapes were placed on the wall of the testing room. Additional cues (vertical and horizontal stripes) were also placed beneath the Barnes maze, visible to mice through the holes. In this open environment, mice naturally seek a dark enclosed place provided by a black goal box (8 cm × 23 cm × 4 cm) under one of the holes. Aversive bright light (~1000 lux) was turned on during the trials.

Mice were randomly assigned to one out of four escape hole locations, invariant throughout the experiment. On the first habituation day, for each of two trials, mice were placed near the goal box and left for 3 min. If a mouse did not escape into the goal box, it was gently guided there and left for 60 s. During each acquisition trial (four trials per day for 4 days), mice were released in the center of the maze and given 3 min to enter the escape hole. On the day after the training period, for the probe trial, the goal box was removed and mice were allowed to move freely for 60 s. Behavioral parameters were recorded using EthoVision XT-10 (Noldus Information Technology). Weighted mean distance was calculated according to the formula: $\sum[d_e] \times n_e / \sum n_{total}$, where d_e = distance moved to the escape hole; n_e = number of nose pokes into the escape hole; and n_{total} = total number of nose pokes into all holes.

Object Recognition

The novel object recognition test is based on the tendency of mice to explore a novel object rather than a familiar one. It was performed essentially as described (Sik *et al*, 2003). At 1 h after an acquisition session exposing mice to two identical objects, mice were placed back in the testing arena in which one of the familiar objects remained and the other was replaced with a novel object. The time examining each object was recorded for 5 min by EthoVision XT-10 and expressed as a percentage of the total time of object exploration. The displaced object recognition procedure was conducted essentially as described (Ng *et al*, 2009). At 2–3 min after an acquisition session to two identical objects, mice were assessed for exploration time to the same two objects, one remaining in the same location and the second displaced to the opposite corner of the testing arena. Further details are provided in the Supplementary Data.

RESULTS

Calsyntenin-2 Deletion Results in Loss of Functional Inhibitory Synapses and Parvalbumin Interneurons

To assess the roles of calsyntenin-2 in brain development and cognitive function, we generated targeted *Clstn2*$^{-/-}$ mice (Supplementary Figure S1). Loss of calsyntenin-2, with no change in expression of other calsyntenins, was confirmed by western blotting of brain homogenates (Figure 1a)

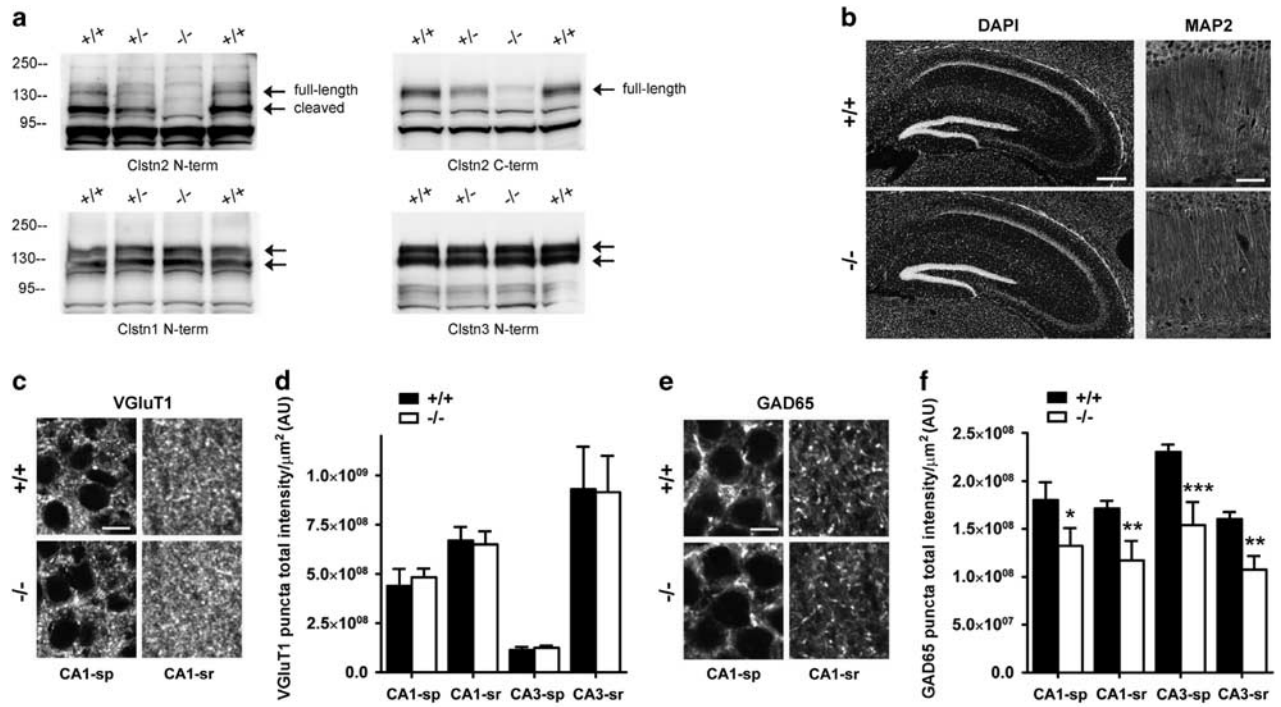

Figure 1 *Clstn2* $^{-/-}$ mice show reductions of an inhibitory but not excitatory synaptic marker. (a) Western blot analysis of post-nuclear brain samples reveals loss of calsyntenin-2 in *Clstn2*$^{-/-}$ mice but no change in the levels of other calsyntenins. The signal remaining with the C-terminal antibody (arrow) likely represents other calsyntenins (Supplementary Figure S1). Note the gene dosage effect on calsyntenin-2 expression in the heterozygous brain. (b) *Clstn2*$^{-/-}$ mice showed no gross anatomical differences from WT, as shown here in hippocampal regions with DAPI nuclear stain, and in CA1 regions with immunofluorescence staining for the dendritic marker microtubule associated protein 2 (MAP2). Scale bars, 200 μm (left) and 50 μm (right). (c, d) VGluT1 puncta immunofluorescence was unaltered in hippocampal regions of *Clstn2*$^{-/-}$ mice. Two-way repeated measures (RM) ANOVA, no genotype effect, $F_{(1,16)} = 0.0041$, $P = 0.95$. Scale bar, 10 μm. (e, f) GAD65 puncta immunofluorescence was reduced in all regions analyzed in *Clstn2*$^{-/-}$mice. Two-way RM ANOVA, genotype effect $F_{(1,8)} = 92.0$, $P < 0.0001$ and $^{*}P < 0.05$, $^{**}P < 0.01$ and $^{***}P < 0.001$ by Bonferroni *post hoc* test comparing with WT for the same region. Scale bar, 10 μm. sp, stratum pyramidale; sr, stratum radiatum; AU, arbitrary units.

with custom made antibodies (Supplementary Figure S2). N-terminal calsyntenin antibodies detected two bands corresponding to full-length proteins and the large cleaved ectodomains. Although full-length and cleaved calsyntenins 1 and 3 were detected in roughly equal amounts in adult brain, calsyntenin-2 was detected mainly as the large cleaved ectodomain with little full-length protein (Figure 1a). Mice lacking calsyntenin-2 showed no obvious deficits in survival or fertility. The gross brain morphology of *Clstn2*$^{-/-}$ mice appeared normal (Figure 1b), as did the overall organization of the excitatory synapse marker VGluT1 and the inhibitory synapse marker glutamic acid decarboxylase GAD65. However, quantitative high-resolution confocal analysis of hippocampal CA1 and CA3 regions revealed significant reductions in GAD65 but not VGluT1 punctate immunofluorescence in adult mice lacking calsyntenin-2 as compared to WT littermate controls (Figure 1c–f). This GABAergic synaptic marker was reduced by 26–33% across brain regions analyzed in *Clstn2*$^{-/-}$ as compared with WT mice.

To determine if the inhibitory synaptic transmission was altered in the absence of calsyntenin-2, we performed whole-cell patch voltage-clamp recordings from CA1 pyramidal neurons in adult *Clstn2*$^{-/-}$ and WT acute hippocampal slices. Compared with WT littermates, there was a significant reduction in the frequency of miniature inhibitory post-synaptic currents (mIPSCs; corresponding to an increased inter-event interval) in *Clstn2*$^{-/-}$ hippocampal slices, with no change in amplitude (Figure 2a–c). No significant differences were detected in mEPSC amplitude or frequency between *Clstn2*$^{-/-}$ mice and WT littermates (Figure 2d–f). Taken together with the imaging data, these results indicate that calsyntenin-2 is selectively required for generating or maintaining normal inhibitory GABAergic functional synapse density *in vivo*.

Among the chemical classes of GABAergic synapses, parvalbumin-positive terminals are particularly abundant as inputs to hippocampal stratum pyramidale and have a prominent role in cognitive function in health and disease (Hu *et al*, 2014; Marin, 2012; Somogyi and Klausberger, 2005). Thus we assessed the density of parvalbumin-positive terminals and found a reduction by 26–40% in CA1 and CA3 stratum pyramidale of *Clstn2*$^{-/-}$ compared with WT mice (Figure 3a and b). This reduction in parvalbumin-positive terminals could result from a deficit in parvalbumin-positive neuron numbers or a deficiency in their development. Counts of parvalbumin-positive neurons revealed reduced numbers per area in hippocampal CA1, CA3, and dentate gyrus, and reduced density in neocortex, by 25–56% (Figure 3c and d). To determine whether all interneuron classes are affected by loss of calsyntenin-2, we assessed interneurons immunoreactive for other markers (Figure 3c–g). There was no difference between *Clstn2*$^{-/-}$ and WT mice in the number of somatostatin-positive neurons in any of these brain regions. Similarly, the density of calretinin-positive neurons in hippocampal CA1, CA3 and neocortex, and of calbindin-positive neurons in hippocampal CA1

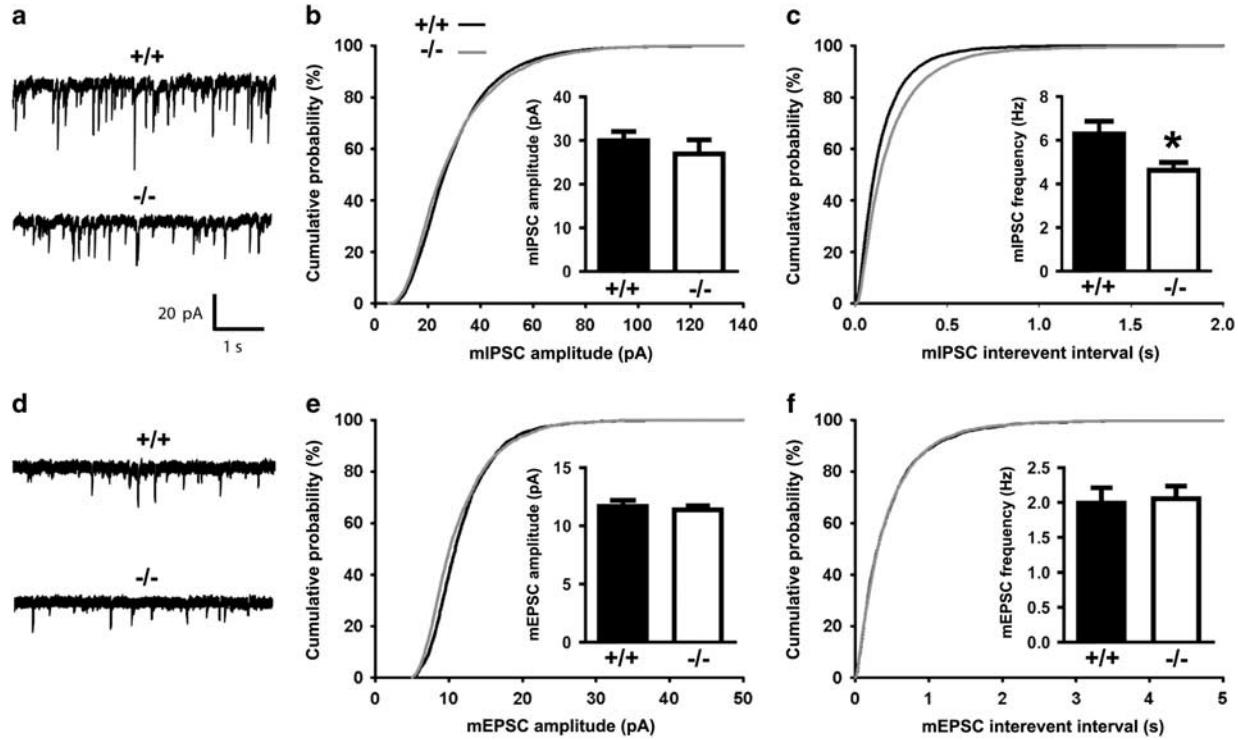

Figure 2 Inhibitory synaptic transmission is reduced in CA1 pyramidal neurons of *Clstn2*$^{-/-}$ mice. (a) Representative mIPSC recordings from hippocampal CA1 pyramidal neurons in acute slices from *Clstn2*$^{-/-}$ and WT adult mice. (b, c) Cumulative distributions of mIPSC amplitude (b) and inter-event intervals (c) in *Clstn2*$^{-/-}$ and WT neurons (Kolmogorov–Smirnov test, $P<0.001$ for inter-event intervals). Insets display mean ± SEM for mIPSC amplitude (b) and frequency (c). mIPSC frequency but not amplitude was significantly reduced in *Clstn2*$^{-/-}$ neurons (Student's *t*-test, $^*P<0.05$; $n=10$ cells for *Clstn2*$^{-/-}$ and 8 cells for WT). (d) Representative mEPSC recordings from hippocampal CA1 pyramidal neurons. (e, f) Cumulative distributions of mEPSC amplitude (e) and inter-event intervals (f) in *Clstn2*$^{-/-}$ and WT neurons. Insets display mean ± SEM for mEPSC amplitude (e) and frequency (f). No significant differences were detected in mEPSCs between groups ($n=8$ cells for *Clstn2*$^{-/-}$ and 9 cells for WT).

and neocortex, were indistinguishable between *Clstn2*$^{-/-}$ and WT mice (the other regions could not be assessed due to immunoreactivity from dentate gyrus hilar or granule cells, respectively). Thus, loss of calsyntenin-2 leads to a selective and widespread loss of parvalbumin-positive interneurons.

Calsyntenin-2 Deletion Results in Hyperactivity and Deficits in Spatial Learning and Memory

Because loss of parvalbumin neurons is associated with psychiatric disorders (Marin, 2012) and *CLSTN2* variants are linked to cognitive function (Jacobsen *et al*, 2009; Pantzar *et al*, 2014; Papassotiropoulos *et al*, 2006), we next tested *Clstn2*$^{-/-}$ mice in an array of behavioral assays. Tests were chosen to assess locomotor activity (open field), anxiety (elevated plus maze), behavioral despair (forced swim test), and multiple forms of learning and memory (Morris water maze, Barnes maze, novel object recognition, and displaced object recognition). *Clstn2*$^{-/-}$ and *Clstn2*$^{+/-}$ mice showed increased locomotor activity in the open field as compared with littermate WT mice (Figure 4a). The fraction of time spent in the center of the open field, an index reflecting anxiety in this task, was comparable between the genotypes (Figure 4a). Furthermore, there were no differences in behavior in the elevated plus maze or forced swim test, indicating that the hyperactivity seen in the open field was not because of changes in anxiety or behavioral despair (Figure 4b and c).

To test learning and memory in *Clstn2*$^{-/-}$ mice, we first used the Morris water maze assay. There was no difference in latency to reach a visible platform between *Clstn2*$^{-/-}$ and WT mice (Student's *t*-test, $t_{(17)}=0.80$, $P=0.44$, $n=9$–10 mice per group) nor in swim speed (*t*-test, $P=0.37$). However, collectively over the training period the mutant mice took a longer time than WT to find the hidden platform (Figure 5a). A behavioral deficit related to spatial memory was observed in the subsequent probe trial, in which *Clstn2*$^{-/-}$ mice spent significantly less time in the target quadrant than WT mice (Figure 5b).

In another spatial learning and memory assay, the Barnes maze, WT mice typically entered the goal box immediately upon the first nose poke into the goal box, whereas *Clstn2*$^{-/-}$ mice exhibited a larger number of nose pokes into the goal box before entering the goal box (Figure 5c). In keeping with this finding, perhaps related to their hyperactivity as assessed in the open field, *Clstn2*$^{-/-}$ mice exhibited a longer latency to enter the goal box (Figure 5c) and longer total distance traveled (two-way repeated measures (RM) ANOVA genotype effect $F_{(1,\ 20)}=26.6$, $P<0.001$; training effect $F_{(3,\ 60)}=11.9$, $P<0.001$) relative to WT mice during all training days. Importantly, the latency to the first nose poke into the goal box was indistinguishable between *Clstn2*$^{-/-}$ and WT mice, and diminished over days of training (Figure 5c). Similarly, distance travelled until the

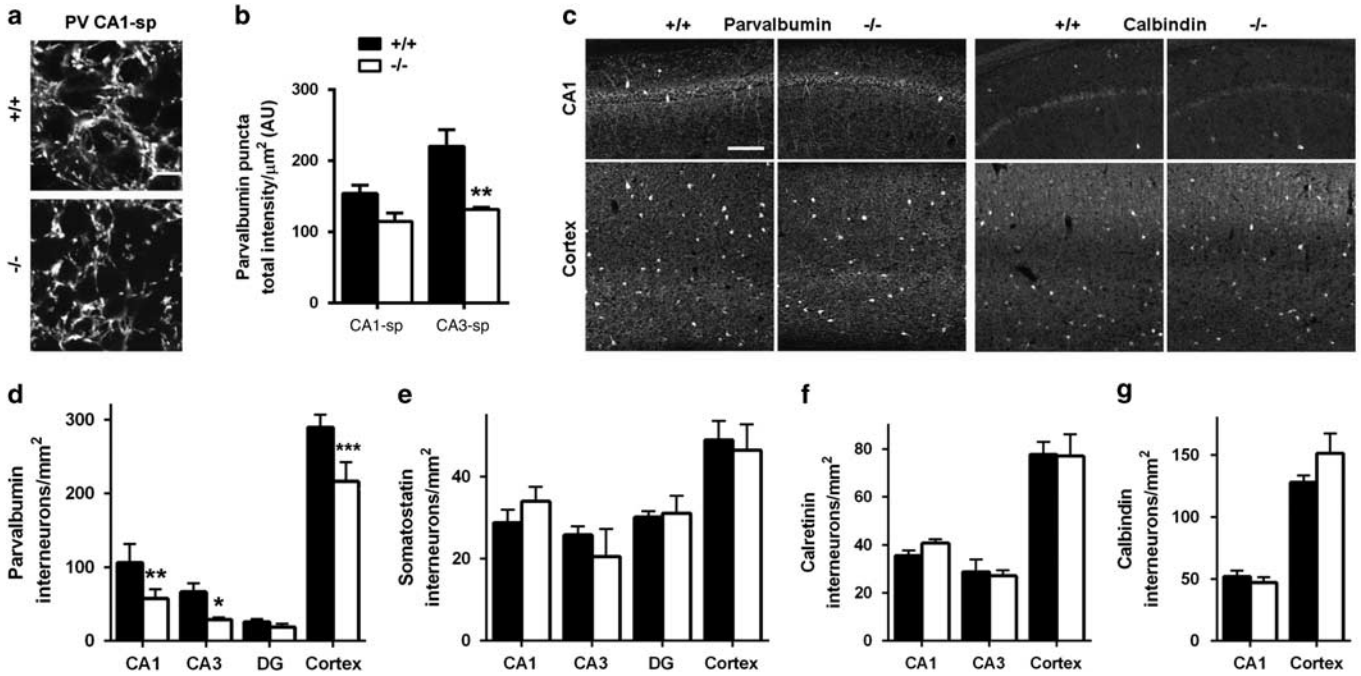

Figure 3 Parvalbumin-positive interneurons are selectively reduced in *Clstn2*$^{-/-}$ mice. (a, b) Parvalbumin (PV) punctate immunofluorescence was reduced in hippocampal regions of *Clstn2*$^{-/-}$ mice (sp, stratum pyramidale). Two-way RM ANOVA, genotype effect $F_{(1,6)} = 20.0$, $P = 0.0042$ and $^{**}P < 0.01$ by Bonferroni *post hoc* test comparing with WT. Scale bar, 20 μm. (c) Sample immunofluorescence in hippocampal CA1 and cortex showing reduced numbers of parvalbumin-positive but not calbindin-positive interneurons in *Clstn2*$^{-/-}$ as compared with WT mice. Scale bar, 100 μm. (d) The number of parvalbumin-positive interneurons was reduced in multiple brain regions of *Clstn2*$^{-/-}$ mice. For each region, all laminae were included in the cell counts. For cortex, the primary motor cortex region was analyzed. Two-way RM ANOVA, genotype effect $F_{(1,16)} = 50.4$, $P < 0.0001$ and $^{*}P < 0.05$, $^{**}P < 0.01$, and $^{***}P < 0.001$ by Bonferroni *post hoc* test comparing with WT for the same region. (e–g) The numbers of somatostatin, calretinin and calbindin immunopositive interneurons were unaltered in *Clstn2*$^{-/-}$ mice. Two-way ANOVA, no genotype effect $F_{(1,40)} = 0.019$, $P = 0.89$ (somatostatin), $F_{(1,29)} = 0.056$, $P = 0.82$ (calretinin), $F_{(1,16)} = 1.03$, $P = 0.33$ (calbindin).

first nose poke into the goal box was indistinguishable between *Clstn2*$^{-/-}$ and WT mice, and diminished over days of training (genotype effect $F_{(1,20)} = 0.20$, $P > 0.05$; training effect $F_{(3,60)} = 2.96$, $P < 0.05$). Thus, *Clstn2*$^{-/-}$ mice learned the spatial location of the goal box equally well. However, in the subsequent probe trial, *Clstn2*$^{-/-}$ mice spent a lower percentage of time in the target quadrant, made a smaller percentage of correct nose pokes into the goal box, and exhibited a larger weighted distance to target than WT mice (Figure 5d). These results confirm a deficit in spatial memory in *Clstn2*$^{-/-}$ mice.

We then assessed *Clstn2*$^{-/-}$ mice in a non-spatial learning and memory task, novel object recognition. Like WT mice, *Clstn2*$^{-/-}$ mice spent more time investigating a novel object than a familiar object (Figure 5e). In the displaced object recognition task, two familiar objects are presented but one is displaced relative to its original position, introducing a spatial component. In this assay, like the WT mice, *Clstn2*$^{-/-}$ mice spent more time investigating the displaced object (Figure 5f). Thus, *Clstn2*$^{-/-}$ mice exhibited selective cognitive deficits in the Morris water maze and Barnes maze tasks but not in novel or displaced object recognition.

The deficits in spatial learning and memory and hyperactivity observed in *Clstn2*$^{-/-}$ mice were all confirmed with a second independent cohort. Again, travel distance in the open field was greater for *Clstn2*$^{-/-}$ than WT mice (Student's *t*-test, $t_{(18)} = 6.91$, $P < 0.0001$, $n = 9$–11 mice per group). In the Morris water maze, *Clstn2*$^{-/-}$ mice again showed an increased time to reach the hidden platform during training (two-way RM ANOVA, genotype effect $F_{(1,17)} = 63.0$, $P < 0.0001$; training effect $F_{(3,54)} = 86.8$, $P < 0.0001$; $n = 10$–12 mice per group) and spent less time in the target quadrant in the probe trial after the training phase (Student's *t*-test, $t_{(20)} = 2.39$, $P = 0.027$). In the Barnes maze, during training *Clstn2*$^{-/-}$ mice again exhibited a longer latency to enter the goal box than WT mice (two-way RM ANOVA, genotype effect $F_{(1,20)} = 25.7$, $P < 0.001$; training effect $F_{(3,60)} = 7.37$, $P < 0.01$, $n = 10$–12 mice per group) but a similar latency to the first nose poke into the goal box (genotype effect $F_{(1,20)} = 0.26$, $P > 0.05$; training effect $F_{(3,60)} = 7.30$, $P < 0.01$). In the subsequent probe trial, *Clstn2*$^{-/-}$ mice again spent a lower percentage of time in the target quadrant (Student's *t*-test, $t_{(20)} = 5.13$, $P < 0.0001$), made a smaller percentage of correct nose pokes into the goal box ($t_{(20)} = 3.34$, $P = 0.003$), and exhibited a larger weighted distance to target than WT mice ($t_{(20)} = 2.83$, $P = 0.011$).

DISCUSSION

In this study, we generated a *Clstn2*$^{-/-}$ mouse model and found the mutant mice to be deficient in spatial learning and memory in the Morris water maze and Barnes maze tasks (Figure 5a–d). These results confirm the proposed role of calsyntenin-2 in hippocampus-dependent learning based on allele association of *CLSTN2* with episodic memory in humans (Papassotiropoulos *et al*, 2006), and in line with data on calsyntenin-2 function in *C. elegans* (Hoerndli *et al*, 2009). *Clstn2*$^{-/-}$ mice performed normally in some cognitive

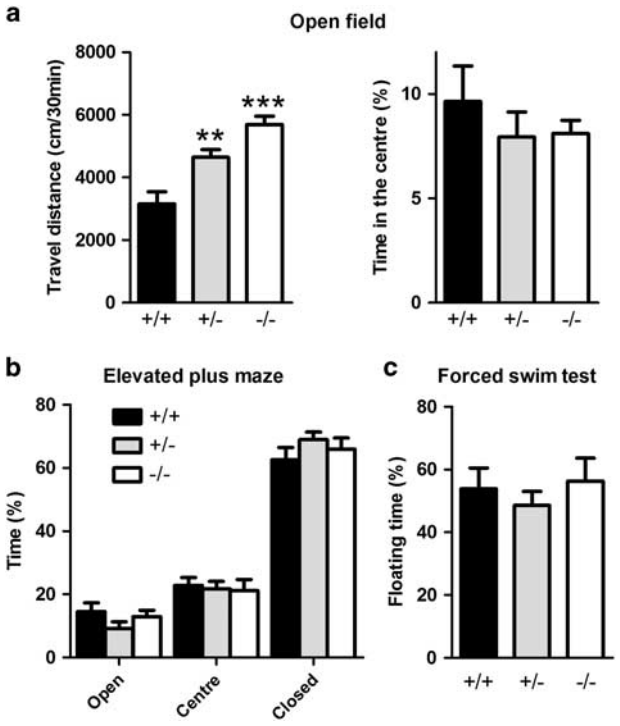

Figure 4 *Clstn2*$^{-/-}$ mice show hyperactivity but no differences in anxiety or depression related behaviors. (a) *Clstn2*$^{-/-}$ and *Clstn2*$^{+/-}$ mice showed increased locomotor activity in the open field (assessed by travel distance) as compared with WT. One-way ANOVA, $F_{(2,\ 27)}=16.3$, $P<0.0001$, and $^{**}P<0.05$, $^{***}P<0.001$ by Bonferroni *post hoc* test comparing with WT; $n=9$–11 mice per group. Mice of all genotypes spent a similar amount of time in the center of the open field ($F_{(2,\ 27)}=0.98$, $P>0.05$). (b) There was no effect of genotype on percent of time spent in each arm in the elevated plus maze. Two-way ANOVA, effect of genotype $F_{(2,\ 81)}=0.0000014$, $P=1.0$, effect of compartment $F_{(2,\ 81)}=309.1$, $P<0.0001$, interaction $F_{(4,\ 81)}=1.12$, $P=0.35$, $n=8$–13 mice per group. Nor was there any effect of genotype on total number of entries into each arm, number of passages from one enclosed arm to another, number of head-dips, number of risk assessment postures, or the number of explorations of an open arm end (not shown; all $P>0.10$). (c) There was no difference between genotypes in the forced swim test. One-way ANOVA, $F_{(2,\ 27)}=0.48$, $P=0.62$, $n=8$–13 mice per group.

tasks, specifically in novel and displaced object recognition (Figure 5e and f), but showed increased locomotor activity in the open field (Figure 4a). These behavioral changes in *Clstn2*$^{-/-}$ mice are not likely to be related to depression-like or anxiety features as the behavior of *Clstn2*$^{-/-}$ mice was indistinguishable from WT in the forced swim test and elevated plus maze test (Figure 4b and c). These phenotypic changes are likely related to the observed reduction in density of parvalbumin-positive interneurons, of inhibitory synaptic markers, and of functional inhibitory synapses in *Clstn2*$^{-/-}$ mouse hippocampus compared with WT (Figures 1, 2 and 3). The normal mIPSC amplitude indicates that the basal synaptic strength of the remaining inhibitory synapses is unaltered in *Clstn2*$^{-/-}$ mice, as are the density and basal strength of excitatory synapses (Figure 2).

Thus a common structure affected in all calsyntenin-deficient mice is the synapse, although different synapse types are involved, with calsyntenin-1 loss affecting excitatory synapses (Ster *et al*, 2014), calsyntenin-2 affecting inhibitory synapses (Figures 1 and 2), and calsyntenin-3 affecting both synapse types (Pettem *et al*, 2013). The observed reductions in punctate terminal immunofluorescence of GAD65 (Figure 1e and f) and parvalbumin (Figure 3a and b) and in density of parvalbumin-positive neurons (Figure 3c and d) upon deletion of calsyntenin-2 likely reflect loss of a subset of inhibitory neurons and synapses. The parvalbumin immunofluorescence signal is robust, and the same antibody as used here was recently used to show that other manipulations can alter parvalbumin expression level per neuron without altering the number of parvalbumin-positive neurons (Donato *et al*, 2013). In *Clstn2*$^{-/-}$ mice, loss of parvalbumin-positive neurons is likely a primary phenotype, leading to a reduction in inhibitory synapses. Further work will be needed to determine the molecular mechanisms by which calsyntenin-2 controls interneuron density, for example, by affecting parvalbumin neuron proliferation, migration, differentiation, maturation, or survival. Thus, although calsyntenin-3 regulates synapse development by binding to presynaptic α-neurexins (Pettem *et al*, 2013), calsyntenin-2 may alter synapses by a more indirect mechanism, by controlling numbers of parvalbumin interneurons.

Consistent with the association of *CLSTN2* alleles with episodic memory in humans, *Clstn2*$^{-/-}$ mice consistently showed impairment in remembering goal locations, both in the Morris water maze and in the Barnes maze. Both of these tasks examine hippocampus-dependent spatial reference memory (Barnes, 1979; Morris *et al*, 1982; Riedel *et al*, 1999). The Barnes maze is less stressful than the Morris water maze (Harrison *et al*, 2009). Limited motivating stress in the Barnes maze, together with the apparent hyperactive phenotype of *Clstn2*$^{-/-}$ mice, may explain why the mutant mice exhibited a larger number of correct pokes and longer escape latency as compared with WT mice. In another spatial task, displaced object recognition, *Clstn2*$^{-/-}$ mice performed equally well as WT littermates, which is intriguing but explainable as several studies have shown a double dissociation between performance in the Morris water maze and displaced object recognition. For example, lateral entorhinal cortex lesions impair performance in the displaced object recognition task but not in the Morris water maze (Van Cauter *et al*, 2013), and medial entorhinal cortex lesions impair performance in the Morris water maze (Hales *et al*, 2014) but can spare behavior in the displaced object recognition task (Van Cauter *et al*, 2013). The involvement of the hippocampus in novel object recognition is debated, and may depend on the particular parameters including the interval between sampling and test (Cohen and Stackman, 2015). Our confocal and functional analyses revealed a role for calsyntenin-2 in inhibitory synapse development in hippocampus, and the reduction in parvalbumin interneurons indicates a similar function in cortex. Although further work will be needed to understand the regional contribution of calsyntenin-2 to performance in the tasks mentioned above, behavioral deficits are likely to be a result of the reduction in parvalbumin neurons and inhibitory synaptic transmission.

Other mouse models that exhibit a reduced density of interneurons, particularly of parvalbumin-positive neurons, share some behavioral characteristics with *Clstn2*$^{-/-}$ mice. *Cntnap2*$^{-/-}$ mice, in which the density of multiple interneuron classes is reduced, exhibit hyperactivity (Penagarikano *et al*, 2011). *En2*$^{-/-}$ mice, in which a subset

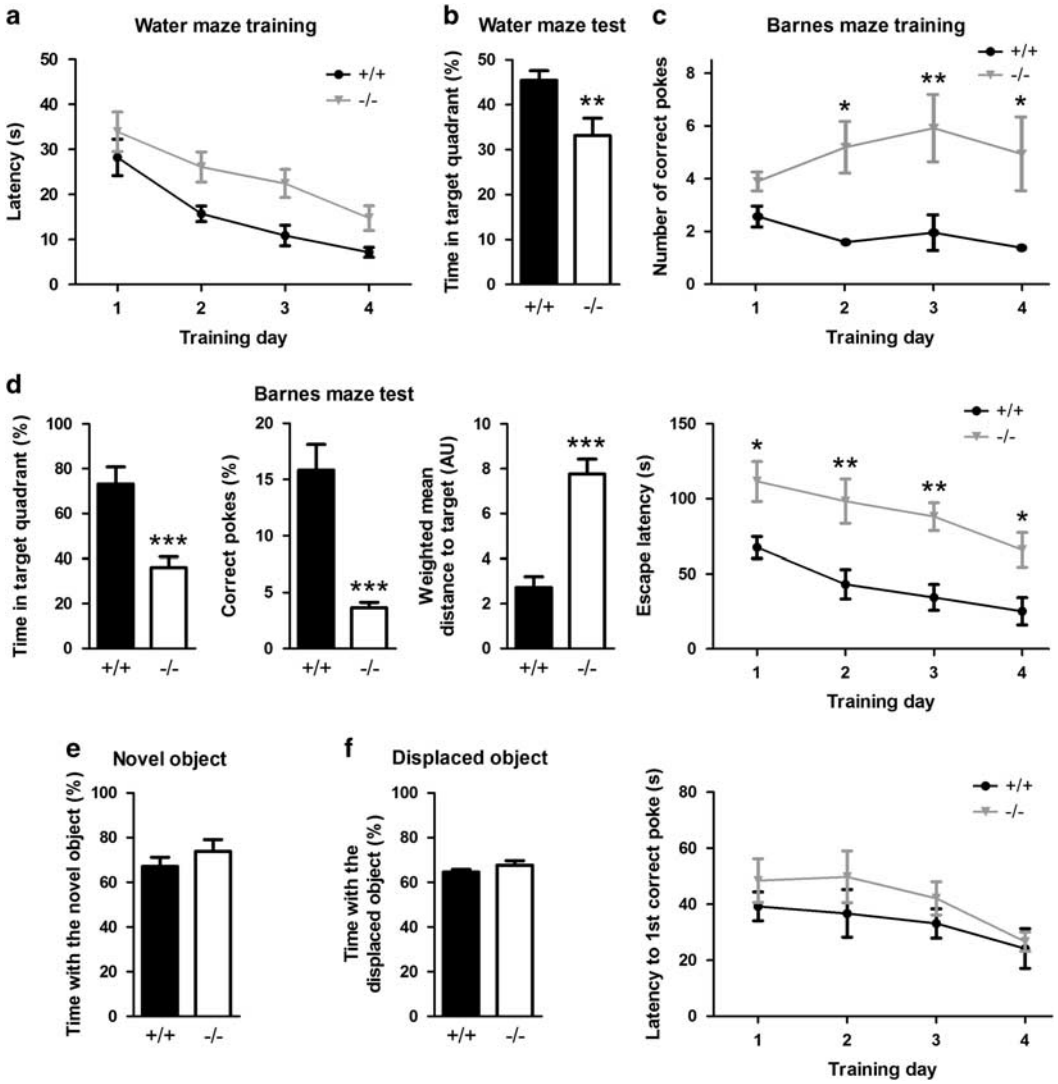

Figure 5 *Clstn2*$^{-/-}$ mice have selective deficits in spatial learning and memory. (a) In the Morris water maze, *Clstn2*$^{-/-}$ mice showed an increased time to reach the hidden platform. Two-way RM ANOVA, genotype effect $F_{(1,17)}=10.6$, $P=0.0046$; training effect $F_{(3,51)}=11.4$, $P<0.0001$; $n=9$–11 mice per group. (b) *Clstn2*$^{-/-}$ mice showed an associated memory deficit in the Morris water maze, indicated by reduced time spent in the target quadrant in the probe trial after the training phase. Student's *t*-test, $t_{(17)}=2.87$, $^{**}P=0.011$. (c) In the Barnes maze training sessions, *Clstn2*$^{-/-}$ mice made a larger number of correct nose pokes than WT before entering the goal box (two-way RM ANOVA genotype effect $F_{(1,20)}=16.3$, $P<0.001$ and $^{*}P<0.05$, $^{**}P<0.01$ by Bonferroni *post hoc* test, $n=10$–12 mice per group). *Clstn2*$^{-/-}$ mice showed a longer escape latency than WT (genotype effect $F_{(1,20)}=39.8$, $P<0.001$ and $^{*}P<0.05$, $^{**}P<0.01$ by Bonferroni *post hoc* test; training effect $F_{(3,60)}=9.37$; $P<0.01$). Yet *Clstn2*$^{-/-}$ mice learned the location of the goal box as shown by no difference from WT in latency to the first correct nose poke (genotype effect $F_{(1,20)}=0.20$, $P>0.05$; training effect $F_{(3,60)}=2.96$, $P<0.05$). (d) *Clstn2*$^{-/-}$ mice showed a memory deficit in the Barnes maze probe test, assessed by time in the target quadrant (Student's *t*-test, $t_{(20)}=4.30$, $^{***}P=0.0003$), percentage of correct nose pokes ($t_{(20)}=5.69$, $^{***}P<0.0001$), or weighted mean distance to target ($t_{(20)}=5.93$, $^{***}P<0.0001$). (e) In the novel object recognition test, *Clstn2*$^{-/-}$ mice spent an equal fraction of time as WT mice exploring the novel object (Student's *t*-test, $t_{(19)}=0.99$, $P=0.33$, $n=10$–11 mice per group). (f) In the displaced object recognition test, *Clstn2*$^{-/-}$ mice spent an equal fraction of time as WT mice exploring the displaced object (Student's *t*-test, $t_{(19)}=1.34$, $P=0.20$, $n=10$–11 mice per group).

of interneurons including parvalbumin-positive cells are reduced, show a learning deficit in the Morris water maze (Brielmaier *et al*, 2012; Sgado *et al*, 2013). *Git1*$^{-/-}$ mice, that show reduced numbers of parvalbumin-positive terminals, but not of somatostatin, calretinin, or calbindin immunopositive terminals, show hyperactivity and a learning deficit in the Morris water maze (Won *et al*, 2011). Finally, an overlapping phenotypic spectrum is also found in mice with parvalbumin neuron-specific deletion of *ErbB4* (Shamir *et al*, 2012). These phenotypic similarities between genetically unrelated mutants at the synaptic/cellular and behavioral levels indicate that the inhibitory drive provided by parvalbumin-positive interneurons is a major determinant of cognitive behavior in mice, which is in line with their assumed role in many neuropsychiatric disorders.

FUNDING AND DISCLOSURE

This work was supported by the National Institutes of Health (MH070860; AMC), a Canada Research Chair salary award (AMC), the German Research Foundation

(SPP1365/KA3423/1-1; HK and NB), the Fritz Thyssen Foundation (HK), the European Union (IMI EU-AIMS; NB), and a Brain Canada Postdoctoral Fellowship (SAC). The authors declare no conflict of interest.

ACKNOWLEDGMENTS

We thank Nazarine Fernandes for excellent technical assistance and Konstantin Pavlov for skillful assistance with EthoVision.

REFERENCES

Araki Y, Kawano T, Taru H, Saito Y, Wada S, Miyamoto K *et al* (2007). The novel cargo Alcadein induces vesicle association of kinesin-1 motor components and activates axonal transport. *Embo J* **26**: 1475–1486.

Araki Y, Miyagi N, Kato N, Yoshida T, Wada S, Nishimura M *et al* (2004). Coordinated metabolism of Alcadein and amyloid beta-protein precursor regulates FE65-dependent gene transactivation. *J Biol Chem* **279**: 24343–24354.

Barnes CA (1979). Memory deficits associated with senescence: a neurophysiological and behavioral study in the rat. *J Comp Physiol Psychol* **93**: 74–104.

Brielmaier J, Matteson PG, Silverman JL, Senerth JM, Kelly S, Genestine M *et al* (2012). Autism-relevant social abnormalities and cognitive deficits in engrailed-2 knockout mice. *PLoS One* **7**: e40914.

Cohen SJ, Stackman RW Jr (2015). Assessing rodent hippocampal involvement in the novel object recognition task. A review. *Behav Brain Res* **285**: 105–117.

Donato F, Rompani SB, Caroni P (2013). Parvalbumin-expressing basket-cell network plasticity induced by experience regulates adult learning. *Nature* **504**: 272–276.

Hales JB, Schlesiger MI, Leutgeb JK, Squire LR, Leutgeb S, Clark RE (2014). Medial entorhinal cortex lesions only partially disrupt hippocampal place cells and hippocampus-dependent place memory. *Cell Rep* **9**: 893–901.

Han S, Tai C, Jones CJ, Scheuer T, Catterall WA (2014). Enhancement of inhibitory neurotransmission by GABAA receptors having alpha2,3-subunits ameliorates behavioral deficits in a mouse model of autism. *Neuron* **81**: 1282–1289.

Harrison FE, Hosseini AH, McDonald MP (2009). Endogenous anxiety and stress responses in water maze and Barnes maze spatial memory tasks. *Behav Brain Res* **198**: 247–251.

Hintsch G, Zurlinden A, Meskenaite V, Steuble M, Fink-Widmer K, Kinter J *et al* (2002). The calsyntenins–a family of postsynaptic membrane proteins with distinct neuronal expression patterns. *Mol Cell Neurosci* **21**: 393–409.

Hoerndli FJ, Walser M, Frohli Hoier E, de Quervain D, Papassotiropoulos A, Hajnal A (2009). A conserved function of C. elegans CASY-1 calsyntenin in associative learning. *PLoS ONE* **4**: e4880.

Hu H, Gan J, Jonas P (2014). Interneurons. Fast-spiking, parvalbumin(+) GABAergic interneurons: from cellular design to microcircuit function. *Science* **345**: 1255263.

Ikeda DD, Duan Y, Matsuki M, Kunitomo H, Hutter H, Hedgecock EM *et al* (2008). CASY-1, an ortholog of calsyntenins/alcadeins, is essential for learning in *Caenorhabditis elegans*. *Proc Natl Acad Sci USA* **105**: 5260–5265.

Jacobsen LK, Picciotto MR, Heath CJ, Mencl WE, Gelernter J (2009). Allelic variation of calsyntenin 2 (CLSTN2) modulates the impact of developmental tobacco smoke exposure on mnemonic processing in adolescents. *Biol Psychiatry* **65**: 671–679.

Kohannim O, Hibar DP, Stein JL, Jahanshad N, Hua X, Rajagopalan P *et al* (2012). Discovery and replication of gene influences on brain structure using LASSO regression. *Front Neurosci* **6**: 115.

Konecna A, Frischknecht R, Kinter J, Ludwig A, Steuble M, Meskenaite V *et al* (2006). Calsyntenin-1 docks vesicular cargo to kinesin-1. *Mol Biol Cell* **17**: 3651–3663.

Laukka EJ, Lovden M, Herlitz A, Karlsson S, Ferencz B, Pantzar A *et al* (2013). Genetic effects on old-age cognitive functioning: a population-based study. *Psychol Aging* **28**: 262–274.

Marin O (2012). Interneuron dysfunction in psychiatric disorders. *Nat Rev Neurosci* **13**: 107–120.

Morris RG, Garrud P, Rawlins JN, O'Keefe J (1982). Place navigation impaired in rats with hippocampal lesions. *Nature* **297**: 681–683.

Ng D, Pitcher GM, Szilard RK, Sertie A, Kanisek M, Clapcote SJ *et al* (2009). Neto1 is a novel CUB-domain NMDA receptor-interacting protein required for synaptic plasticity and learning. *PLoS Biol* **7**: e41.

Pantzar A, Laukka EJ, Atti AR, Papenberg G, Keller L, Graff C *et al* (2014). Interactive effects of KIBRA and CLSTN2 polymorphisms on episodic memory in old-age unipolar depression. *Neuropsychologia* **62C**: 137–142.

Papassotiropoulos A, Stephan DA, Huentelman MJ, Hoerndli FJ, Craig DW, Pearson JV *et al* (2006). Common Kibra alleles are associated with human memory performance. *Science* **314**: 475–478.

Penagarikano O, Abrahams BS, Herman EI, Winden KD, Gdalyahu A, Dong H *et al* (2011). Absence of CNTNAP2 leads to epilepsy, neuronal migration abnormalities, and core autism-related deficits. *Cell* **147**: 235–246.

Pettem KL, Yokomaku D, Luo L, Linhoff MW, Prasad T, Connor SA *et al* (2013). The specific alpha-neurexin interactor calsyntenin-3 promotes excitatory and inhibitory synapse development. *Neuron* **80**: 113–128.

Preuschhof C, Heekeren HR, Li SC, Sander T, Lindenberger U, Backman L (2010). KIBRA and CLSTN2 polymorphisms exert interactive effects on human episodic memory. *Neuropsychologia* **48**: 402–408.

Riedel G, Micheau J, Lam AG, Roloff EL, Martin SJ, Bridge H *et al* (1999). Reversible neural inactivation reveals hippocampal participation in several memory processes. *Nat Neurosci* **2**: 898–905.

Saab BJ, Saab AM, Roder JC (2011). Statistical and theoretical considerations for the platform re-location water maze. *J Neurosci Methods* **198**: 44–52.

Sgado P, Genovesi S, Kalinovsky A, Zunino G, Macchi F, Allegra M *et al* (2013). Loss of GABAergic neurons in the hippocampus and cerebral cortex of Engrailed-2 null mutant mice: implications for autism spectrum disorders. *Exp Neurol* **247**: 496–505.

Shamir A, Kwon OB, Karavanova I, Vullhorst D, Leiva-Salcedo E, Janssen MJ *et al* (2012). The importance of the NRG-1/ErbB4 pathway for synaptic plasticity and behaviors associated with psychiatric disorders. *J Neurosci* **32**: 2988–2997.

Sik A, van Nieuwehuyzen P, Prickaerts J, Blokland A (2003). Performance of different mouse strains in an object recognition task. *Behav Brain Res* **147**: 49–54.

Somogyi P, Klausberger T (2005). Defined types of cortical interneurone structure space and spike timing in the hippocampus. *J Physiol* **562**: 9–26.

Ster J, Steuble M, Orlando C, Diep TM, Akhmedov A, Raineteau O *et al* (2014). Calsyntenin-1 regulates targeting of dendritic NMDA receptors and dendritic spine maturation in CA1 hippocampal pyramidal cells during postnatal development. *J Neurosci* **34**: 8716–8727.

Van Cauter T, Camon J, Alvernhe A, Elduayen C, Sargolini F, Save E (2013). Distinct roles of medial and lateral entorhinal cortex in spatial cognition. *Cereb Cortex* **23**: 451–459.

Won H, Mah W, Kim E, Kim JW, Hahm EK, Kim MH *et al* (2011). GIT1 is associated with ADHD in humans and ADHD-like behaviors in mice. *Nat Med* **17**: 566–572.

Supplementary Information accompanies the paper on the Neuropsychopharmacology website (http://www.nature.com/npp)